Performance Assessment of Distributed Communication Architectures in Smart Grid

Jing Jiang, and Hongjian Sun
School of Engineering and Computing Sciences
Durham University, Durham DH1 3LE, UK
Email: { jing.jiang, hongjian.sun} @durham.ac.uk

***Abstract*— The huge amount of smart meters and growing frequent data readings have become a big challenge on data acquisition and processing in smart grid advanced metering infrastructure systems. This requires a distributed communication architecture in which multiple distributed meter data management systems (MDMSs) are deployed and meter data are processed locally. In this paper, we present the network model for supporting this distributed communication architecture and propose to use large-scale antenna array at the distributed MDMSs to further improve communication performance. We provide performance assessment for this architecture in terms of system throughput and cost efficiency. Specifically, we derive a closed-form asymptotic approximation to the system throughput, which exhibits a very good accuracy compared with simulation results. Based on this tight approximation, we have defined cost efficiency, which takes the deployment cost of distributed MDMSs into account. Our results demonstrate the significant advantages of the distributed architecture over the transitional centralized one in terms of communication performance and scalability. By carefully selecting the number of distributed MDMSs, the distributed communication architecture is also cost efficient.**

Keywords— smart grid; advanced metering infrastructure; distributed communication architecture; large-scale antenna array.

I. Introduction

Smart grid (SG) has been introduced as a modernized electrical grid that integrates information and communication technologies for improving the efficiency, reliability, economics, and sustainability of the electricity distribution and management [1]. An effective, scalable, and reliable communication architecture is the key to achieving potential advantages of the SG.

The traditional communication architecture for smart grid is constructed in a centralized topology where information is delivered to and processed at a centralized control center. Taking advanced metering infrastructure (AMI) into account, it is a system that acquires metering data, delivers them to a data concentrator and then to a meter data management system (MDMS), and analyze them using analytical tools at MDMS [2]. This traditional centralized architecture is a simple architecture and easy to manage. However, with the number of smart meters increasing or the system scale increasing, it is highly likely that this centralized communication architecture reaches its physical limit of handling these data and can no longer meet the service requirements in terms of data rates, latency and reliability, which will cause data congestion, serious latency, or even data loss. Such effects can significantly impair SG services. In addition, the data collection frequency (i.e., every 15 minutes) has been discussed to improve further (e.g. in a 30 second interval) in achieving advanced SG functionalities [3]. In consequence, a larger amount of metering data will need to be delivered to and processed at MDMS, which will cause a greater burden to the AMI communication architecture. To sum up, the vast amount of smart meters, growing frequent data readings, and handling of large-scale meter data have posed a big challenge on the scalability of SG communication architecture.

Distributed communication architectures have been proposed to provide efficient smart grid AMI services in facing fast growing traffic from smart meters [3-5]. In [3], Zhou et al. proposed a distributed communication architecture for SG systems that has some similarities with the content distribution network (CDN) in which multiple distributed MDMSs are deployed and connected to a central MDMS. In [4], a multi-level distributed architecture was introduced, in which metering data is aggregated and processed in a tree-like manner. We share the same motivations as in [3]; but we note that the achievable data rate on each concentrator is highly relevant to the transmission distance, which is not constant as used in [3]. The paper's main contributions are summarized as follows:

- Firstly, we present the network model for supporting the distributed communication architecture; we propose to use large-scale antenna array at the distributed MDMS to further improve communication performance.
- Secondly, we analyze the system throughput and provide a closed-form approximation on it; the approximation exhibits a very good accuracy. Results show that the system throughput will be significantly improved by using the distributed communication architecture.
- Thirdly, we define cost efficiency to capture the additional cost for deploying corresponding equipment for distributed MDMSs; we demonstrate to what extent the distributed architecture can obtain benefits in terms of cost efficiency.

The rest of this paper is organized as follows. Section II specifies the distributed communication architecture. The system performance assessment is analyzed in Section III. Simulation results are shown in Section IV, and Section V concludes the paper.

II. DISTRIBUTED COMMUNICATION ARCHITECTURE

In this Section, we will introduce the distributed communication architecture for supporting AMI in SG.

A. A Scalable Distributed Communication Architecture

The proposed scalable distributed communication architecture for supporting AMI is shown in Fig. 1, where multiple distributed MDMSs are deployed with each distributed MDMS serving one local area. The operation and management functionalities enabled by MDMS include geographic information system (GIS), consumer information system (CIS), distribution management system (DMS), outage management system (OMS) and asset management systems (AMS), etc. [3]. This architecture consists of two layers:

- In the lower layer (with public or private communications), each distributed MDMS is communicated with several data concentrators via wireless links, and the metering data is stored and processed locally at the specified distributed MDMS. Compared to the centralized architecture, the required communication distance for the distributed architecture is largely shortened and thus the information will be delivered more stably and efficiently.

- In the upper layer (with private communications), the distributed MDMS communicates with the central MDMS through a backbone network. Most operations and managements can be done at the distributed MDMS, that is, only summarized information needs to be transmitted to the central MDMS. The communication resource needed between the central MDMS and distributed MDMSs can be viewed as almost constant.

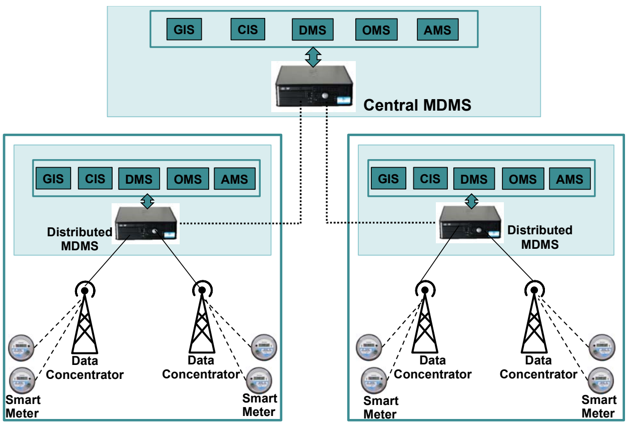

Fig. 1. A distributed AMI communication architecture in smart grid

Since the distributed communication architecture is planned to provide communication coverage for the smart meters in a large area, the locations of distributed MDMSs should be well planned. We note that the coverage of the smart grid AMI area and the locations of the data concentrators are normally accessible as prior knowledge for designing the locations of distributed servers. We propose to use Voronoi tessellation, which is optimal in the sense of minimizing average transmission distances from the data concentrators to the distributed MDMSs [6]. To realize this Voronoi tessellation, the Linde–Buzo–Gray algorithm is used.

B. Communication Technologies Used for the Distributed Architecture

For the upper layer communications, we propose to use fiber-optic, which is a mature and stable wired communication technology, to provide high-speed, high-secure, and reliable communications between the distributed MDMSs and the central MDMS. For the lower layer communications, wireless technologies can be used to reap the benefits of quick deployment, well standardizations, widespread access and greater flexibility [7]. For example, WiMAX and cellular network communications (3G or 4G) can provide wireless communication solutions for distributed MDMSs communicating with data concentrators.

As one of the advanced communication techniques, massive multiple-input and multiple-output (MIMO) technique can also be used in the proposed communication architecture to further improve communication performance [8]. The idea of massive-MIMO is that very large number of low-power antennas located at a base station node or distributed geographically transmits concentrated beams (instead of broadcasting signals to cover the entire area) to the users concurrently and in the same frequency band [9]. The massive MIMO technique has the benefits of eliminating many random effects (e.g. uncorrelated noise and small-scale fading) and thus leading to higher data rates and reliable communication. We propose to use massive MIMO and employ large-scale low-power antennas at the distributed server base stations.

III. PERFORMANCE EVALUATIONS

A. Problem Formulation

We consider that in one local region where the i-th distributed MDMS is deployed, the distributed MDMS is equipped with M-antenna and the value of M is large. The total number of distributed MDMSs is N. In the i-th region, the distributed MDMS communicates with K_i single-antenna data concentrators, that is, $\sum_{i=1}^{N} K_i = K$. The communication between the distributed MDMS and data concentrators is operated on a time-division duplexing mode with channel reciprocity [9]. The received signal y_{im} at the m-th data concentrator in the i-th cell can be expressed as

$$y_{im} = \sqrt{P_t}\, \boldsymbol{g}_{im}^{H} \boldsymbol{s}_i + n_{im}. \tag{1}$$

The M-by-1 vector $\boldsymbol{g_{im}}$ represents the uplink channel from the m-th data concentrator to the i-th distributed MDMS, and P_t denotes the average transmit power at the distributed server. We model the channel vector as $\boldsymbol{g}_{im} = \boldsymbol{\Phi}_{im}^{1/2} \boldsymbol{h}_{im}$, where $\boldsymbol{h}_{im}$ is the independent fast fading vector in which components are independent and identically distributed (i.i.d.) and have circularly-symmetric complex Gaussian random distribution with unit variance and zero mean. The M-by-M matrix $\boldsymbol{\Phi}_{im}$ denotes the long-term channel statistics. For a common channel model, i.e. a centralized massive MIMO system with all antennas co-located at the base station, we have

$$\boldsymbol{\Phi}_{im} = \left(K_t d_{im}^{\zeta}\right)^{-1} \Theta_{im}, \tag{2}$$

where $\mathbf{\Theta}_{im}$ represents the spatial correlation matrix at the distributed MDMS side, d_{im} is the distance from the i-th distributed MDMS to the m-th data concentrator, ζ is the path loss exponent, and K_t is a constant indicating the physical characteristics of the channel and the power amplifier [10]. In addition, the M-by-1 vector $\boldsymbol{s_i}$ in (1) represents the transmit vector at the i-th distributed MDMS, which can be given as $\boldsymbol{s_i} = \boldsymbol{W_i x_i}$, where $\boldsymbol{W_i} = [\boldsymbol{w_1} \cdots \boldsymbol{w_{K_i}}]$ is a M-by-K_i precoding matrix and the K_i -by-1 vector $\boldsymbol{x_i} = [x_1 \cdots x_{K_i}]^{\mathbf{T}} \sim \mathcal{CN}(0, \boldsymbol{I_{K_i}})$ contains the data symbols intended for the data concentrators. The scalar $n_{im} \sim \mathcal{CN}(0, \sigma^2)$ is the additive white Gaussian noise (AWGN) at the receiver, and σ^2 denotes the noise variance.

B. Achievable Data Rates and Asymptotic Analysis

We consider matched filter (MF) pre-coder, at the distributed MDMS, and have $\boldsymbol{W_i} = \boldsymbol{G_i} = [\boldsymbol{g_{i1}} \cdots \boldsymbol{g_{iK_i}}]$. The ergodic achievable rate of the m-th data concentrator is

$$R_{im} = B_i \mathbb{E}[\log_2(1 + \gamma_{im})], \tag{3}$$

where $\mathbb{E}[\cdot]$ denotes the expectation operation and B_i is the communication bandwidth per data concentrator in cell i, and $\boldsymbol{\gamma}_{im}$ is the signal-to-interference-plus-noise ratio (SINR) which is given by

$$\boldsymbol{\gamma}_{im} = \frac{\mathbb{E}\left[|\boldsymbol{g}_{im}^{\mathrm{H}} \boldsymbol{g}_{im}|^2 \right]}{\mathbb{E}\left[\frac{\boldsymbol{\sigma}^2}{P_t} |\boldsymbol{g}_{im}|^2 + \sum_{l=1, l \neq m}^{K_i} |\boldsymbol{g}_{il}^{\mathrm{H}} \boldsymbol{g}_{im}|^2 \right]}. \tag{4}$$

As the massive MIMO technique is used, we consider the system where M grows infinitely large. We use the asymptotic analysis to provide approximations for finite M and K_i. Now we derive deterministic approximations $\tilde{\gamma}_{im}$ of the SINR γ_{im}, such that $\gamma_{im} - \tilde{\gamma}_{im} \xrightarrow[M\to\infty]{a.s.} 0$ where $\xrightarrow{a.s.} 0$ denotes almost sure convergence. According to the continuous mapping theorem of convergent sequences [11], we have

$$R_{im} - B_i \log_2(1 + \tilde{\boldsymbol{\gamma}}_{im}) \xrightarrow[M\to\infty]{a.s.} 0. \tag{5}$$

Proposition 1: Consider a local region where an M-antenna distributed MDMS communicates with K_i data concentrators; The massive MIMO technique is deployed; Suppose that the long-term channel matrices are uniformly bounded with respect to M, i.e., $\limsup_{M\to\infty} \sup_{1\le m\le K_i} \|\mathbf{\Phi}_m\| < \infty$. Then we have

$$\tilde{\boldsymbol{\gamma}}_{im} = \left(\mathrm{tr}\boldsymbol{\Phi}_{im}\right)^2 \Big/ \left[\frac{\boldsymbol{\sigma}^2}{P_t} \mathrm{tr}\boldsymbol{\Phi}_{im} + \sum_{l=1}^{K_i} \mathrm{tr}\boldsymbol{\Phi}_{im}\boldsymbol{\Phi}_{il} \right]. \tag{6}$$

Proof: To prove this proposition, we first recall several preliminary results on large random matrices: Let $\boldsymbol{A} \in \mathbb{C}^{\boldsymbol{M}\times\boldsymbol{M}}$ be deterministic and $\boldsymbol{Z} \in \mathbb{C}^{\boldsymbol{M}\times\boldsymbol{M}}$ be a random vector of independent entries. Suppose that $\boldsymbol{z} \sim \mathcal{CN}(0, \boldsymbol{I}_M/M)$ and $\boldsymbol{A}$ is uniformly bounded with respect to M. For $p \geq 1$, we have

$$\boldsymbol{z}^{\mathrm{H}}\boldsymbol{A}\boldsymbol{z} - \frac{1}{M}\mathrm{tr}\boldsymbol{A} \xrightarrow[M\to\infty]{a.s.} 0; \quad \mathbb{E}\left[\left| \boldsymbol{z}^{\mathrm{H}}\boldsymbol{A}\boldsymbol{z} - \frac{1}{M}\mathrm{tr}\boldsymbol{A} \right|^p \right] = \mathcal{O}\left(\frac{1}{M^{p/2}} \right). \tag{7}$$

Since the MF detector is considered, we have (4). Dividing the denominator and numerator of $\boldsymbol{\gamma}_{im}$ by $1/M^2$ and using (7), the computation of signal power yields

$$\frac{1}{M^2}\mathbb{E}\left[|\boldsymbol{g}_{im}^{\mathrm{H}}\boldsymbol{g}_{im}|^2 \right] = \mathbb{E}\left[\left| \frac{1}{M}\boldsymbol{h}_{im}^{\mathrm{H}}\boldsymbol{\Phi}_{im}\boldsymbol{h}_{im} \right|^2 \right] \xrightarrow[M\to\infty]{a.s.} \left(\frac{1}{M}\mathrm{tr}\boldsymbol{\Phi}_{im} \right)^2. \tag{8}$$

Then for the noise and interference power, we have

$$\frac{1}{M^2}\mathbb{E}\left[\sum_{l=1, l\neq m}^{K_i} \boldsymbol{g}_{il}^{\mathrm{H}}\boldsymbol{g}_{im}\boldsymbol{g}_{im}^{\mathrm{H}}\boldsymbol{g}_{il} \right] \xrightarrow[M\to\infty]{a.s.} \frac{1}{M^2}\sum_{l=1}^{K} \mathrm{tr}\boldsymbol{\Phi}_{im}\boldsymbol{\Phi}_{il}. \tag{9}$$

We add one term $(\mathrm{tr}\mathbf{\Phi}_{im}^2) / M^2$ in (9) which can be neglected for large M. Inserting (8) and (9) into (4), we thus have (6). This completes the proof.

From (5) and (6), we have a straightforward understanding of the achievable rate for one data concentrator

$$R_{im} - B_i \log_2\left(1 + \frac{\left(\mathrm{tr}\boldsymbol{\Phi}_{im}\right)^2}{\frac{\boldsymbol{\sigma}^2}{P_t}\mathrm{tr}\boldsymbol{\Phi}_{im} + \sum_{l=1}^{K_i}\mathrm{tr}\boldsymbol{\Phi}_{im}\boldsymbol{\Phi}_{il}} \right) \xrightarrow[M\to\infty]{a.s.} 0. \tag{10}$$

We will now illustrate the effect of transmission distance on the achievable rate for one data concentrator and to what extent the distributed communication architecture can benefit the communication performance. When we consider the channels between the i-th distributed MDMS and data concentrators are statistically i.i.d., we have

$$\boldsymbol{\Phi}_{im} = (K_t d_{im}^{\zeta})^{-1}\boldsymbol{\Theta}_{im} = (K_t d_{im}^{\zeta})^{-1}\boldsymbol{I}_M. \tag{11}$$

From Proposition 1, the asymptotic SINR $\tilde{\gamma}_{im}$ can be given by

$$\tilde{\boldsymbol{\gamma}}_{im} = \frac{(K_t d_{im}^{\zeta})^{-1}M^2}{\frac{\boldsymbol{\sigma}^2}{P_t}M + \sum_{l=1}^{K_i}(K_t d_{il}^{\zeta})^{-1}} = \frac{M^2}{\frac{\boldsymbol{\sigma}^2}{P_t}MK_t d_{im}^{\zeta} + d_{im}^{\zeta}\sum_{l=1}^{K_i} d_{il}^{-\zeta}}. \tag{12}$$

The first term of the denominator in (12) is from the effective SNR and the second term is from the interference. Compared to the first term of the denominator, the second term is very small and can be neglected. We thus have a simplified but still tight approximation of the SINR, as follows

$$\tilde{\boldsymbol{\gamma}}_{im} = M \Big/ \left(\frac{\boldsymbol{\sigma}^2}{P_t} K_t d_{im}^{\zeta} \right). \tag{13}$$

We define $\bar{R}_i$ as the average achievable rate on a concentrator and obtain

$$\bar{R}_i = \frac{1}{K_i}\sum_{m=1}^{K_i} B_i \log_2(1 + \tilde{\boldsymbol{\gamma}}_{im}) = \frac{1}{K_i}\sum_{m=1}^{K_i} B_i \log_2\left(1 + \frac{MP_t}{\boldsymbol{\sigma}^2 K_t d_{im}^{\zeta}} \right). \tag{14}$$

To exam the accuracy of the closed-form approximation (14), we consider a simulation scenario that 50 concentrators are uniformly distributed in a 20-by-20 Km area. One MDMS is deployed and communicates with the concentrators. Simulations and approximations of the average achievable rate on a concentrator versus the number of antennas M is shown in

Fig. 2. The figure shows that the proposed asymptotic approximation in (10) and the simplified version (14) are both quite closed to the simulation results for the entire range of M (even when M is not large, i.e. for realistic system dimensions) and thus used for analytically addressing the cost efficiency problem as shown in next subsection.

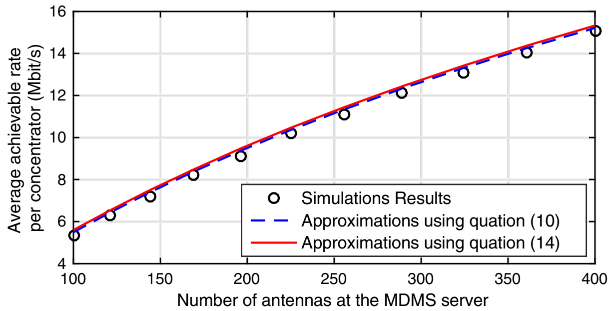

Fig. 2. Comparison of simulations and approximations of the average achievable rate on a concentrator versus the number of antennas M, where 50 concentrators are randomly distributed in 20*20 Km area, ζ=3.5, K_t=10^3, B_i=10 MHz, noise power density is -174 dBm/Hz, P_t= 10 W.

Following (14), the system throughput for the lower layer of the distributed communication system can be given by

$$RD_{\text{sum}} = \sum_{i=1}^{N}\sum_{m=1}^{K_i} B_i \log_2\left(1+\frac{MP_t}{\sigma^2 K_t d_{im}^{\zeta}}\right), \text{ where } \sum_{i=1}^{N} K_i = K. \quad (15)$$

For the convenience of comparison, we also show the system throughput of the traditional central communication system as

$$RS_{\text{sum}} = \sum_{m=1}^{K} B \log_2\left(1+\frac{MP_t}{\sigma^2 K_t d_{cm}^{\zeta}}\right), \quad (16)$$

where d_{cm} is the distance between the concentrator m and the central MDMS.

C. Cost efficiency Evaluations

Even though the proposed distributed communication architecture offer many benefits in terms of scalability and communication performance as discussed in previous sections, it cause additional cost for deploying corresponding equipment for distributed MDMSs. We define C as the constant data rate needed for exchanging information between a distributed MDMS and the central MDMS. As discussed in Section II.B, fiber-optic can be used in the private backhaul network; but it is very expensive. We thus need to consider the additional communication cost and define f as the unit communication cost of the backbone network (€/Mbps/Km). The additional cost for deploying this distributed architecture includes:

- Deployment cost of distributed MDMSs: We define F_d as the cost of deploying a distributed MDMS server in cell i, and F_c as cost of deploying the central MDMS center.
- Communication cost from distributed MDMSs to the central MDMS; refer to the variable f as defined above.

The total cost of the distributed communication architecture is thus given by

$$NF_d + F_c + NfCD, \quad (17)$$

where D is the average distance from a distributed MDMS to the central MDMS in the unit of kilometer. We define the cost efficiency as the achievable system throughput over the total cost (bps/Euro). And from (15) and (16), we have the cost efficiency of the distributed architecture CE_D and that of the central one CE_C as,

$$CE_D = \frac{\sum_{i=1}^{N}\sum_{m=1}^{K_i} B_i \log_2\left[1+MP_t/\sigma^2 K_t d_{im}^{\zeta}\right]}{NF_d + F_c + NfCD}, \text{ where } \sum_{i=1}^{N} K_i = K. \quad (18)$$

$$CE_C = \frac{\sum_{m=1}^{K} B \log_2\left[1+MP_t/\sigma^2 K_t d_{cm}^{\zeta}\right]}{F_c}. \quad (19)$$

IV. Simulation Results and Discussions

We consider a simulation scenario that K=2500 concentrators are uniformly distributed in a 100-by-100 Km area. This simulation scenario corresponds to a city with about 1 million populations and the number of smart meters covered by each concentrator is 100 on average [3]. Distributed MDMSs directly communicate with data concentrators, and report summary power and grid information to the central MDMS via private backhaul networks. The physical channel propagation parameters are adopted from the 3GPP LTE standard models. The channels are modeled as Rayleigh fading channel. The path loss exponent is set to 3.5 to reflect an urban area, and the constant indicating the physical characteristics of the channel and the power amplifier (i.e., K_t) is set to 10^3 [10]. We consider the noise power density as -174 dBm/Hz, and data channel is 10 MHz. We select the Macro type of transmitter and assume P_t= 46 dBm =40 W. The locations of distributed MDMSs are selected via Voronoi tessellation.

The average achievable rate on a concentrator versus the number of distributed MDMSs N is shown in Fig. 3 (a). Two case of M, i.e., 256, 128 antennas per distributed MDMS, are considered and compared. The traditional centralized architecture is also shown in the figure as a special case where N=1. From the figure, we can see that compared to the traditional centralized architecture, the proposed distributed architecture can provide much better communication performance in terms of achievable data rate per concentrator. In other words, with the same data rate requirements, the distributed communication architecture can cover much larger area then the centralized architecture. In addition, the large-scale antenna array deployed at the distributed MDMS can help to improve the communication performance.

Using the above simulation settings, in Fig. 3 (b), we show the total cost of the distributed communication architecture. We consider f = €50 per Mbps×Km, and C = 50 Mbps. For the case of 256 antennas per distributed MDMS, the deployment cost is assumed that F_c= €400,000 and F_d= €200,000. As to the case of 128 antennas per distributed MDMS, the deployment cost is a bit lower; we assume F_c= €380,000 and F_d= €180,000. As expected, the total cost increases dramatically as the number of distributed MDMSs N increases.

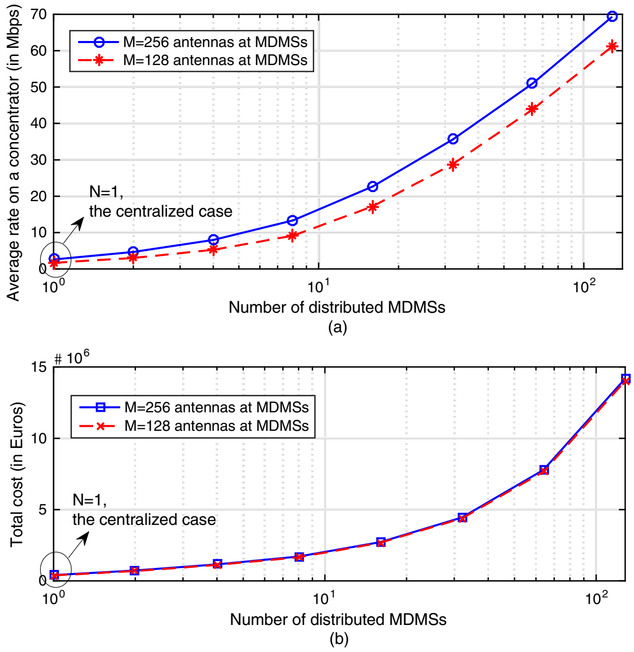

Fig. 3. Average achievable rate on a concentrator and total cost of the distributed communication architecture, where the number of distributed MDMSs N varies, and two cases of M are considered.

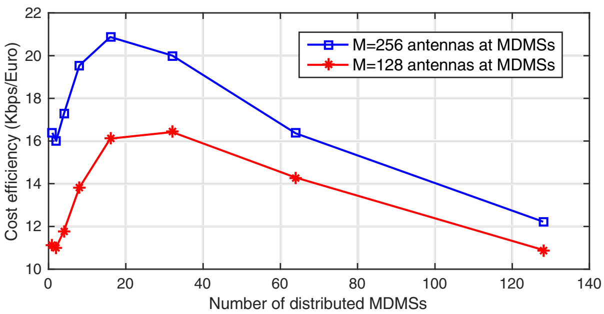

Fig. 4. Cost efficiency of the distributed communication architecture (with unit Kbps/Euro) versus the number of distributed MDMSs N.

Using the total cost shown in Fig. 3 (b), we illustrate the cost efficiency of the distributed communication architecture versus the number of distributed MDMSs N in Fig. 4. The cost efficiency has been defined by equation (20). As shown in Fig. 4, the centralized architecture (with $N = 1$) is a bit more cost efficient than the architecture where 2 distributed MDMSs are used. The reason is that the benefits obtained by the distributed architecture is not sufficient enough to redeem the additional deployment cost when $N = 2$. However, with more number of distributed MDMSs deployed, i.e. with N increasing, cost efficiency of the distributed architecture becomes increasing but finally decreasing. The figure illustrates there exists an optimal region of N in terms of maximizing the cost efficiency, which provides insight for designing the distributed communication architecture in practice.

CONCLUSIONS

In this paper, we have studied the distributed communication architecture to provide efficient smart grid AMI services. We have presented the communication techniques to support this architecture and proposed to use large-scale antenna arrays at the distributed MDMSs. We have analyzed the system throughput and provided a closed-form approximation on it. The approximation exhibits a high level of accuracy compared with simulation results. Based on this tight approximation, we have defined cost efficiency to capture the additional cost of deploying corresponding equipment for this distributed architecture. Our results have demonstrated that the system throughput is significantly improved by using the distributed architecture. That is, at the same data rate requirements, the distributed communication architecture can cover much larger area then the centralized case. Even though deploying such a distributed architecture will cause additional cost, by carefully selecting the number of distributed MDMSs, the distributed architecture is still cost efficient. These performance assessments provide valuable insight for designing the distributed communication architecture in practical smart gird.

ACKNOWLEDGMENT

This work was supported by the European Commission's Horizon 2020 Framework Programme (H2020/2014-2020) under Grant Agreement 646470, SmarterEMC2 Project.

REFERENCES

[1] Q.-D. Ho, Y. Gao, and T. Le-Ngoc, "Challenges and research opportunities in wireless communication networks for smart grid," *IEEE Wireless Communications*, vol. 20, no. 3, pp. 89-95, June 2013.

[2] CEN-CENELEC-ETSI Smart Grid Coordination Group, Smart Grid Reference Architecture, November 2012, online: http://ec.europa.eu/energy/sites/ener/files/documents/xpert_group1_reference_architecture.pdf

[3] J. Zhou, R. Q. Hu, and Y. Qian, "Scalable Distributed Communication Architectures to Support Advanced Metering Infrastructure in Smart Grid," in *IEEE Transactions on Parallel and Distributed Systems*, vol.23, no.9, pp.1632-1642, Sept. 2012.

[4] H. G. Ngo, L. Liquori, and C. H. Nguyen, "A Scalable Communication Architecture for AMI in SmartGrid," *Technical Report*, RR-8410, 2013.

[5] S. Meiling and T. Steinbach and T. C. Schmidt and M. Wa¨hlisch , "A Scalable Communication Infrastructure for Smart Grid Applications using Multicast over Public Networks," in *Proceedings of the 28th Annual ACM Symposium on Applied Computing*, 690-694, 2013.

[6] J. Jiang, J. S. Thompson, H. Sun, "Practical Analysis of Codebook Design and Frequency Offsets Estimation for Virtual-MIMO Systems," *IET Communications*, vol.7, no.6, pp. 585-594, April 16 2013.

[7] H. Sun, A. Nallanathan, B. Tan, J. Thompson, J. Jiang, and H. Poor, "Relaying technologies for smart grid communications," *IEEE Wireless Communications*, vol. 19, no. 6, pp. 52–59, December 2012.

[8] E. Larsson, O. Edfors, F. Tufvesson, and T. Marzetta, "Massive MIMO for next generation wireless systems," *IEEE Commun. Mag.*, vol. 52, no. 2, pp. 186–195, February 2014.

[9] F. Rusek, D. Persson, B.K. Lau, E.G. Larsson, T.L. Marzetta, O. Edfors, F. Tufvesson, et al., "Scaling up MIMO: Opportunities and challenges with very large arrays," *IEEE Signal Processing Mag.*, vol. 30, no. 1, pp. 40–60, Jan 2013.

[10] J. Jiang, M. Dianati, M. Imran, R. Tafazolli, "Energyefficiency analysis and optimization for virtual-MIMO systems," *IEEE Trans. Vehicular Technology*, vol. 63, no. 5, pp. 2272–2283, June 2014.

[11] R. Couillet and M. Debbah, *Random Matrix Methods for Wireless Communications*. Cambridge University Press, 2011.